ASM Handbook, Volume 11, *Failure Analysis and Prevention*
B. Miller, R. Shipley, R. Parrington, D. Dennies, editors
DOI 10.31399/asm.hb.v11.a0006776

Fatigue Fracture Appearances

Ronald J. Parrington, Engineering Systems Inc. (ESi)

FATIGUE FAILURE of engineering components and structures results from progressive fracture caused by cyclic or fluctuating loads. The magnitude of each individual load event is too small to cause complete fracture of the undamaged component, but the cumulative action of numerous load cycles, often numbering in the hundreds of thousands and millions, results in initiation and gradual propagation of a crack or cracks. Complete fracture ensues when the crack reaches a critical size that is dependent on fracture toughness. Fatigue is an important potential cause of mechanical failure, because most engineering components or structures are or can be subjected to cyclic loads during their lifetime.

Fatigue may be categorized as low-cycle fatigue or high-cycle fatigue. Low-cycle fatigue occurs after a relatively low number of cycles, whereas high-cycle fatigue occurs after a relatively high number of cycles. Low-cycle fatigue may involve bulk plasticity and/or more plastic strain at the crack tip, whereas the deformation in high-cycle fatigue is primarily elastic. There is no universally accepted demarcation between low- and high-cycle fatigue. Furthermore, some industry-specific dividing lines between low- and high-cycle fatigue exist. For example, in the aerospace industry low-cycle fatigue is attributed to the thermomechanical stresses associated with engine acceleration and deceleration (i.e., one flight equals one cycle), while high-cycle fatigue is associated with lower-magnitude in-flight vibrations and cyclic stresses. A commonly accepted (albeit arbitrary) dividing line between low- and high-cycle fatigue is approximately 10^4 cycles. For very-low-cycle fatigue or progressive overload failures, those that exhibit gross plastic deformation on the macroscale and occurring after only tens or hundreds of cycles, the microscale fracture surface appearance or morphology may be similar to monotonic ductile overload failures (i.e., microvoid coalescence or dimpled rupture). In general, the discussion of fatigue fracture appearance in this article does not apply to very-low-cycle fatigue failures.

This article focuses on fractography of fatigue. However, it should be noted that fractography is only part of the failure analysis of a fractured component. As with other fracture mechanisms, proper identification of fatigue requires understanding of the fracture behavior of the particular material subject to failure analysis. At least some knowledge of environmental and service conditions is usually necessary. Evaluation of loading conditions, mechanical properties, microstructure, and surface conditions, often in conjunction with fractography, also provides useful information regarding the fundamental cause of failure.

This article begins with an abbreviated summary of fatigue processes and mechanisms. Characteristic fatigue fracture features that can be discerned visually or under low magnification are then described. Typical microscopic features observed on structural metals are presented subsequently, followed by a brief discussion of fatigue in nonmetals. As described in this article, various macroscopic and microscopic features can be used in some situations to characterize the history and growth rate of fatigue. Because fatigue propagation occurs progressively over time, knowledge of inspections performed prior to complete failure can benchmark the time span over which cracking occurred (or can point out inspection deficiencies).

Correlation between mechanical analysis and fractography also can help pinpoint the fundamental cause of fatigue failure. Techniques for predicting fatigue crack initiation, fatigue crack propagation rate, and fatigue life, based on loading conditions in engineering components, are discussed in many texts on applied mechanical engineering, such as Ref 1 and 2. The mechanisms and processes of fatigue are described in more detail in Ref 3. These topics are also addressed in *Fatigue and Fracture*, Volume 19 of the *ASM Handbook*, 1996.

A number of publications provide extensive examples of representative fatigue fractographs (Ref 4–9). This article is not intended to provide a comprehensive atlas of fatigue fracture appearances. While these reference texts are of immense value, the experience of the fractographer remains an important aspect of good failure analysis.

Fatigue Processes

Fatigue has been defined as "the process of progressive localized permanent structural change occurring in a material subjected to conditions that produce fluctuating stresses or strains at some point or points and that may culminate in cracks or complete fracture after a sufficient number of fluctuations" (ASTM E 1150-87, reapproved in 1993). From the perspectives of design, testing, and failure analysis, the fatigue process can be conveniently divided into three parts:

- Crack initiation
- Progressive crack propagation
- Final (fast) fracture

Design and testing aspects of fatigue are discussed in more detail elsewhere, such as in *Fatigue and Fracture*, Volume 19 of the *ASM Handbook*, 1996; and *Mechanical Testing and Evaluation*, Volume 8 of the *ASM Handbook*, 2000. Volume 19 also includes more detailed discussion of the fatigue process than is presented in this article.

As illustrated in Fig. 1, fatigue fractures have one or more fatigue origins (initiation sites), a region of progressive fatigue crack propagation, and a final fast overload fracture

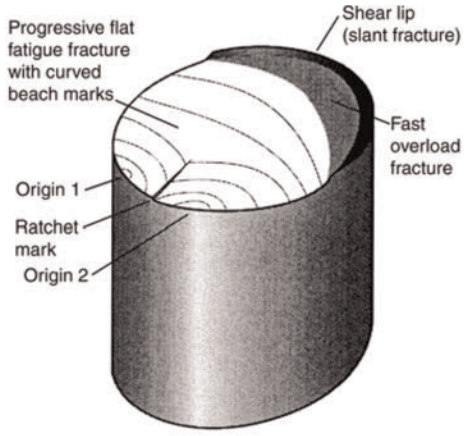

Fig. 1 General features of fatigue fractures

zone. Identification of the location and nature of origin sites is important in failure analysis of fatigue, because fatigue crack initiation is frequently the life-controlling step in the failure process. Discontinuities introduced during processing or manufacture (e.g., abnormally large inclusions, weld discontinuities, grinding cracks) or service (e.g., corrosion pits, impact damage) can result in fatigue crack initiation under circumstances in which an unflawed component would have had acceptable fatigue life. Conversely, inadequate design, excessive load, or low material strength can result in fatigue failure in the absence of a particular "defect" at the origin site. Fractography provides the basis for identifying the fatigue fracture mechanism and for locating origin sites from examination of fracture surfaces.

Initiation of Fatigue

Initiation of fatigue in common components made of commercial alloys occurs at—and is dominated by—material and geometric heterogeneities. Sites fostering fatigue crack initiation include inclusions, second-phase particles, voids, machining marks and other surface flaws, and notches or other geometric variations. These sites can act as stress concentrators or can rapidly produce microcracks by mechanisms such as inclusion debonding and particle fracture. The stress-concentration effect permits local permanent plastic deformation at nominal stresses below yield. Initiation frequently occurs near free surfaces, because nominal stresses are often higher there (e.g., bending and torsion). Geometric variations at surfaces can locally elevate stresses and strains, and processes of damage accumulation (described subsequently for pure unflawed materials) are also favored at surfaces.

Tests made to elucidate mechanisms of initiation frequently have been performed using pure single-phase, relatively homogeneous metals (without the heterogeneities described previously). Based on observations from these tests, some researchers further separate the initiation stage into (Ref 3):

- Accumulation of local irreversible plastic deformation
- Creation of microscopic flaws
- Growth and coalescence of flaws to form one or more macroscopic cracks

Careful laboratory study of unnotched high-purity metals and alloys has shown that repeated plastic deformation can result in localization of permanent microstructural changes. For example, under inelastic cyclic loading, bands of intense slip known as persistent slip bands form in individual crystals of pure face-centered cubic metals such as copper. Fine protrusions and intrusions (peaks and troughs) of metal can form where these persistent slip bands intersect free surfaces (e.g., see Fig. 2 in "Fatigue Failure in Metals" in *Fatigue and Fracture*, Volume 19 of the *ASM Handbook*, 1996). Continued surface roughening and damage accumulation ultimately results in crack nucleation at the surface. Cyclic damage can also accumulate at grain boundaries, particularly at elevated temperature or under conditions that cause grain-boundary embrittlement, and at twin boundaries.

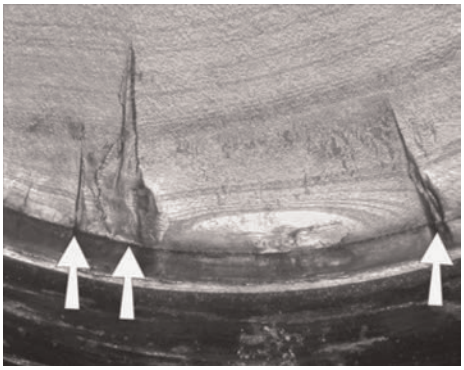

Fig. 2 Close-up view of ratchet marks between distinct surface origin sites in an 18.4 cm (7.25 in.) low-alloy steel shaft that failed in rotating-bending fatigue. Ratchet marks (at arrows) are roughly radial steps formed where fatigue cracks initially propagating on different planes intersected. The ratchet mark at the middle arrow was damaged by postfracture contact.

Propagation

Fatigue crack propagation has been historically divided into two parts, designated stage I and stage II. Stage I propagation occurs on specific crystallographic planes with greatest resolved fluctuating shear stress. Stage II propagation occurs on planes normal to the fluctuating tensile stress. Certain metals (such as aluminum alloys) and loading conditions considered by early researchers investigating fatigue processes exhibited stage I propagation over a limited region (characteristically spanning no more than a few near-surface grains) adjacent to origin sites, followed by a transition to stage II propagation (e.g., see Fig. 16 in "Micromechanisms of Monotonic and Cyclic Crack Growth" in *Fatigue and Fracture*, Volume 19 of the *ASM Handbook*, 1996). Consequently, this division between stages of propagation was a natural one.

However, many commercial alloys (notably most steels) typically do not exhibit any detectable stage I propagation. After initiation in such alloys, growth immediately occurs by so-called stage II propagation. Notches, sharp corners, or preexisting cracks can also eliminate detectable stage I propagation in many metals. In contrast, some alloys (such as certain nickel-base superalloys and cobalt-base alloys) can display very extensive regions of propagation on specific crystallographic planes (so-called stage I propagation) with little or no discernable stage II type of growth prior to final fracture. Depending on loading and geometry, extensive propagation in these materials occurs on alternate crystallographic planes such that growth follows a zigzag or serrated faceted pattern, on average normal to the direction of fluctuating tension.

The stage I propagation mechanism is favored in materials that exhibit planar slip and in some alloys strengthened by coherent precipitates (such as age-hardened aluminum) and under fluctuating loads low enough that the cyclic fracture process zone is small relative to a characteristic microstructural scale parameter. Hence, stage I propagation is often favored by large grain size. Stage II propagation is favored in materials with easy cross slip (wavy slip). In this article, fatigue propagation appearance is described in terms of morphology rather than the didactic separation into stages I and II.

From a practical failure analysis perspective, fatigue crack propagation regions are the most important for identifying the mechanism of failure. While fatigue propagation usually occupies a much larger area than the origin site(s), initiation processes may occupy a significant portion or majority of the overall time (duration) of the fatigue process.

Final Fracture

Final fracture does not occur by a fatigue mechanism at all but is simply fracture caused by the last load application, resulting in complete separation. This final overload fracture may be more or less ductile or brittle, depending on notched or precracked properties of the material (see the articles "Monotonic Overload and Embrittlement" and "Mechanisms and Appearances of Ductile and Brittle Fracture in Metals" in this Volume).

Macroscopic Appearance of Fatigue Fracture

Examination of a fatigue fracture usually begins with unaided visual observation, often followed by viewing with a hand lens or optical stereomicroscope. Macroscopic examination of fracture surfaces can be performed on-site (when the broken part is accessible), requires little or no preparation of the specimen, and uses minimal and relatively simple equipment. It does not destroy the specimen or alter fracture surfaces. Macroscopic examination is particularly useful in correlating fracture surface characteristics with part size and shape and with loading conditions. Fatigue origins are frequently located most readily by viewing the fracture surface at low magnifications (up to 30 to 50×).

Initiation

As previously noted, fatigue fractures often initiate at free surfaces. Stresses are frequently higher at free surfaces, particularly under bending and torsion loading. Geometric stress raisers are often found at surfaces, and processes of fatigue crack initiation are favored by the associated stress concentration. Manufacturing and fabrication processes (e.g.,

welding and machining) can introduce surface irregularities or discontinuities that act as points of stress concentration, facilitating fatigue crack initiation.

In many common situations, such as uniaxial loading of prismatic members and rotating bending of shafts, the driving force for fatigue initiation (e.g., stress range) is relatively uniform over extended volumes or regions. For relatively low driving force, fatigue initiates at one or a few locations within these extended regions or volumes where material resistance is least. Variations in fatigue initiation resistance (in the absence of gross discontinuities) are provided by factors such as variations in grain orientation and variations in inclusion size or shape. In the absence of gross discontinuities, fatigue initiation at low driving force occupies the majority of the total fatigue life.

Circumstances such as relatively high surface driving force can foster numerous crack initiations within a region loaded relatively uniformly. The number of discrete initiation sites tends to increase with increasing driving force. An array of geometric stress raisers can also lead to crack initiation at numerous sites. Multiple-crack initiation rarely results in formation of fatigue cracks that are coplanar. When noncoplanar individual fatigue cracks join together, a ridge or shear ledge is formed between them. Short ridges along a free edge between relatively flat fracture surfaces are called ratchet marks and are indicative of multiple initiation sites (initiation sites are located on both sides of a ratchet mark). They are generally oriented normal to the surface where cracking initiated, at least near the surface. Ratchet marks are often found in fatigue failures, as illustrated in Fig. 1 and 2.

In some situations, fatigue crack initiation does not occur at a free surface. For example, components that have been case hardened, surface hardened, or shot peened can exhibit subsurface initiation. Such surface treatments introduce compressive surface residual stresses (favorable for improving fatigue resistance by reducing the driving force for initiation) and/or increase surface fatigue strength. Under some conditions, these gradients in driving force and resistance result in subsurface fatigue crack initiation (Fig. 3). Figures 4 and 5 illustrate subsurface fatigue initiation in surface-hardened and case-hardened steel components.

Fatigue caused by contact stress, such as rolling-contact loading, also frequently initiates subsurface. As illustrated in Fig. 6, stresses generated by contact between two surfaces characteristically display a maximum shear stress component located beneath the surface. For sufficiently high varying contact stress levels, this can result in subsurface initiation and initial growth of fatigue in shear (Fig. 7). Under contact loading, as sliding increases, fatigue crack initiation sites shift to the surface (Fig. 8). Rolling and sliding contact can cause fatigue damage, such as pitting of gears and spalling of rolls (Fig. 9, 10).

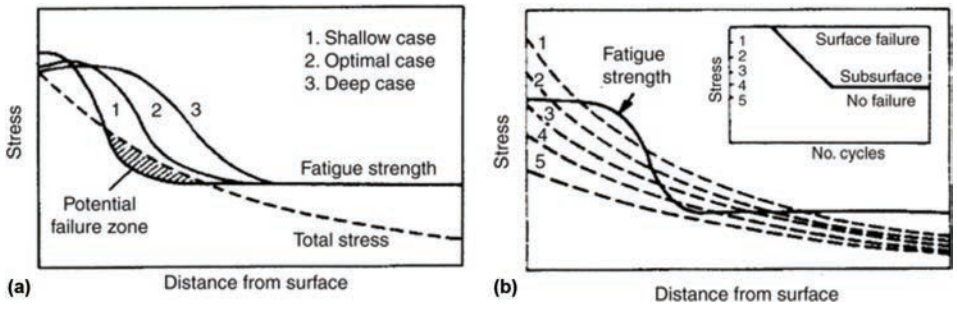

Fig. 3 Schematic of gradients in fatigue initiation driving force (shown as total stress) and fatigue resistance (fatigue strength) that can result in subsurface initiation in a case-hardened component. Total stress includes applied plus residual stress. The surface is located at the left of each diagram. (a) Subsurface initiation occurs for the shallow case because total stress exceeds local fatigue strength in the shaded (subsurface) area. (b) Subsurface initiation occurs for stress curves 3 and 4, while surface initiation is expected for higher-stress levels 1 and 2. Source: Ref 10

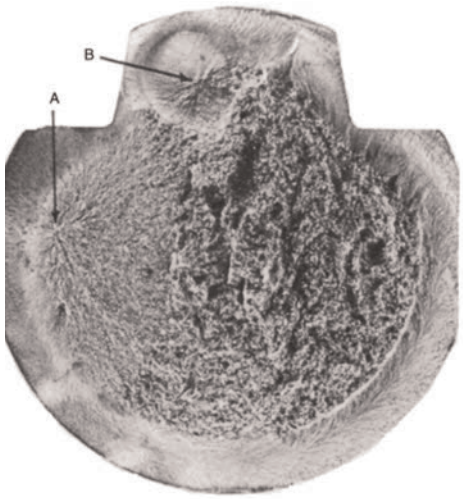

Fig. 4 Subsurface fatigue origins (at arrows) in an induction-hardened 8.25 cm (3.25 in.) high-manganese medium-carbon steel axle laboratory tested in rotating bending. Note absence of beach marks. Source: Ref 11

Fig. 5 Subsurface fatigue origin in-service failure of 6.4 cm (2.5 in.) nitrided medium-carbon alloy steel crank pin. In contrast with the fracture surface shown in Fig. 4, produced in the laboratory under continuous uniform loading, this surface exhibits beach marks. Courtesy of G.J. Fowler, Fowler Inc.

Finally, significant subsurface discontinuities or material defects can foster subsurface fatigue crack initiation, provided sufficient stresses are applied (Fig. 11).

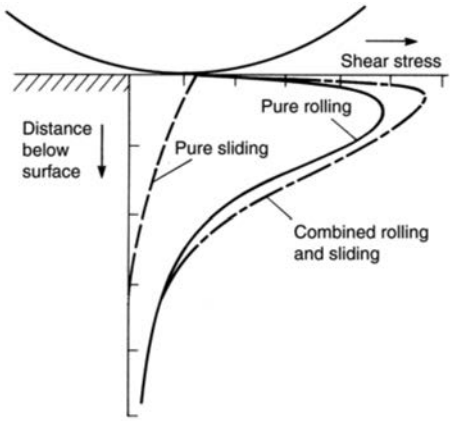

Fig. 6 Schematic illustration of stress distribution associated with rolling contact of a cylindrical member (at top) against a flat surface. The maximum shear stress occurs beneath the surface and can result in subsurface fatigue crack initiation. Source: Ref 12

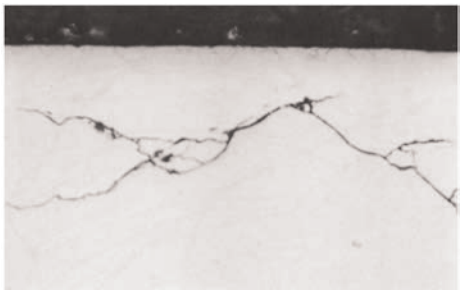

Fig. 7 Unetched metallographic cross section through gear tooth showing subsurface fatigue crack formed by rolling contact. Original magnification: 132×. Source: Ref 12

Propagation

As illustrated in Fig. 1, the progressive crack propagation region of typical components that fail in fatigue is macroscopically flat under axial and/or bending loads. This region is generally transverse to the direction of cyclic or fluctuating tensile stress that caused

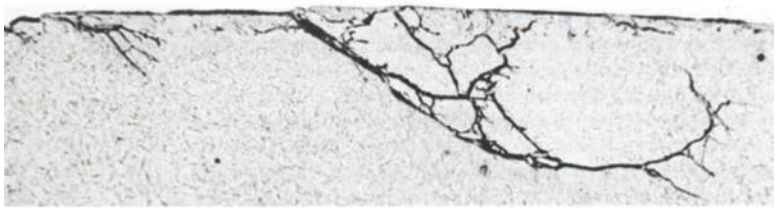

Fig. 8 Unetched metallographic cross section through hardened steel roller test specimen with sliding plus rolling contact (sliding to left and rolling to right). Fatigue cracks initiate at surface. Source: Ref 11

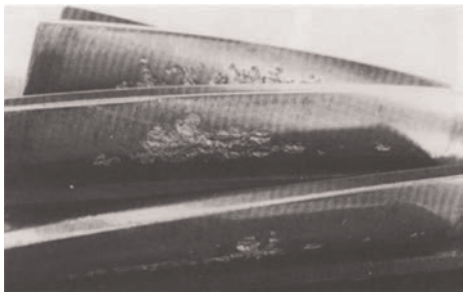

Fig. 9 Pitting on helical gear teeth caused by contact fatigue. Pitting cracks frequently initiate on a subsurface. Source: Ref 12

Fig. 10 Large circular spall on forged, hardened alloy steel mill roll. Faint red arrow marks location of subsurface fatigue origin. Beach marks are evident within the fatigue propagation zone, which is surrounded by fast brittle fracture. Source: Ref 4

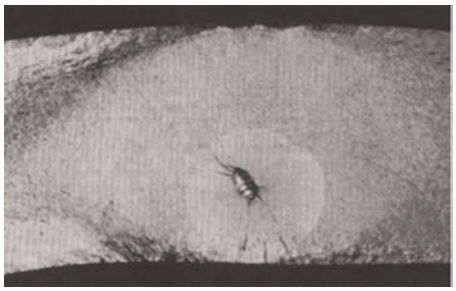

Fig. 11 Subsurface fatigue origin at gross welding discontinuity. Source: Ref 13

fatigue. However, at high loads/high fatigue crack growth rates in relatively thin components made of relatively tough material, a transition to propagation on a slant plane can occur (Fig. 12). Macroscopically, fatigue fracture ordinarily has a brittle appearance and lacks the gross plastic deformation (e.g., necking) characteristic of ductile tensile overload fracture. In contrast with tensile overload fracture, which generally has more-or-less shear lip (slant 45° fracture) along free surfaces, propagating fatigue fractures typically intersect free surfaces at right angles (Fig. 13). This provides a tool for helping to identify fatigue locations (Fig. 14).

Under cyclic or fluctuating torsional loading, fatigue cracks may initiate on planes of maximum shear. Propagation principally occurs on planes normal to the direction of resolved tensile stress (Fig. 15). Figures 16 and 17 present examples of this behavior.

In common with other progressive fracture mechanisms such as stress-corrosion cracking, field fatigue fractures are frequently decorated by more-or-less curved marks that delineate the position of the crack front at a particular point in time. These marks are commonly called beach marks and are also known as clamshell marks and arrest lines or marks. The term *beach marks* is usually reserved for fatigue fractures (i.e., cyclic loading conditions), whereas the term *arrest lines* is appropriate for monotonic (e.g., stress-corrosion cracking) or cyclic loading conditions. Beach marks are produced by a change in crack growth conditions, such as a change in environment or stress level or a pause in stress cycling (interruption in service). Consequently, beach marks are not found in most laboratory tests conducted under uniform loading and environmental conditions (Fig. 4, 13). Examples of beach marks observed on field failures are presented in Fig. 18 and 19. As illustrated in Fig. 20, the presence of arrest lines is consistent with, but is not conclusive evidence of, fatigue fracture. Fracture mechanism identification should also include consideration of factors such as material behavior, service loading and environmental conditions, and microscopic fracture features.

The stress-intensity factor (particularly its cyclic range) characterizes the driving force for fatigue crack propagation of macroscopic cracks growing under conditions of small-scale yielding. The stress-intensity factor is relatively uniform along a straight through-thickness crack in simple components loaded in tension or bending, such as common fracture mechanics specimens. Consequently, under such loading in the small-scale yielding regime, through cracks propagating by fatigue in macroscopically homogeneous materials tend to have relatively straight crack fronts.

Surface or internal flaws and cracks have more-or-less curved crack fronts. For a given

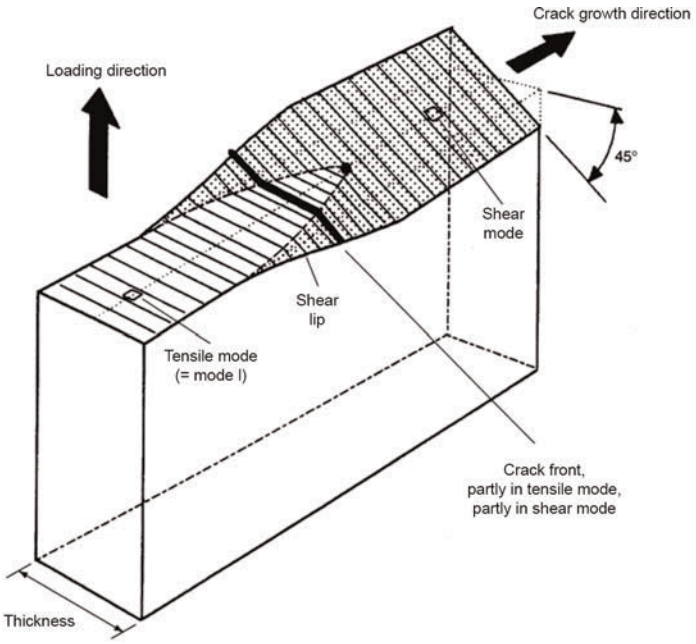

Fig. 12 Schematic illustration of transition from flat (tensile mode) fatigue crack propagation to growth on a slant plane (shear mode). Propagation on a slant plane can occur in relatively thin, tough materials at high growth rates. Source: Ref 14

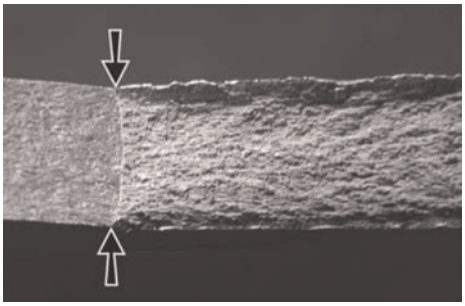

Fig. 13 Aluminum alloy fracture mechanics test specimen, 6.3 mm (0.25 in.) thick. Fatigue crack at left of arrows is flat and perpendicular to side surfaces (note absence of beach marks in this laboratory fatigue fracture). Overload fracture to right of arrows has 45° shear lips extending upward at the top side of the sample and downward at the bottom side.

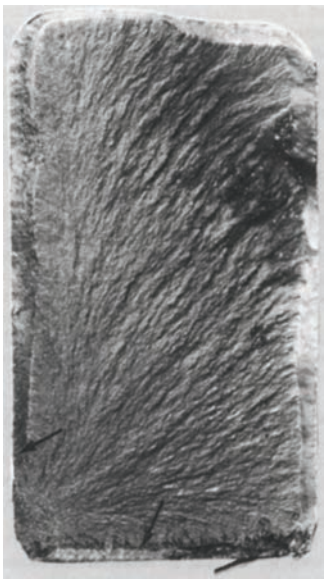

Fig. 14 Fatigue failure of a low-alloy steel part. Shear lips around most of the periphery (as at arrows) as well as radial marks over most of the fracture surface aid in identifying the fatigue fracture area at the lower left corner. Source: Ref 15

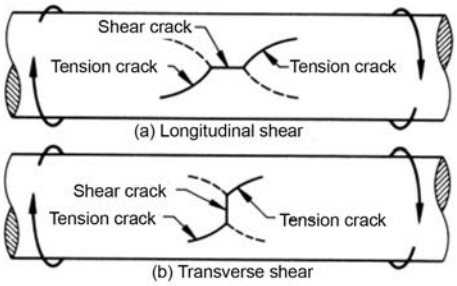

Fig. 15 Schematic illustrations of initiation and early stages of propagation of fatigue cracks in rods subjected to torsion. Fatigue can initiate on planes of maximum shear (longitudinal or transverse), then propagate under cyclic or fluctuating tensile stress acting at 45° to the circular rod axis. An X-pattern can form under reversed torsional loading. Source: Ref 15

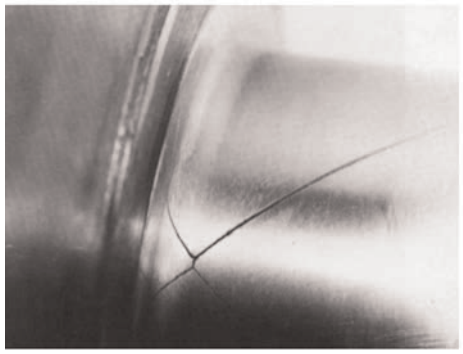

Fig. 16 Characteristic X-pattern on the surface of a medium-carbon steel crankshaft tested under reversed torsional fatigue. Fatigue initiated on a transverse plane of maximum shear, then propagated on two pair of helical surfaces. Source: Ref 11

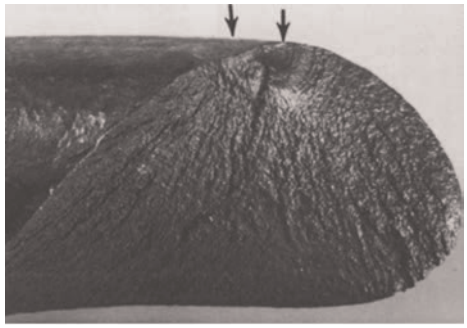

Fig. 17 Torsional fatigue failure of boron-containing alloy steel helical spring. Fatigue initiated at an abraded area marked by arrows. The material in compression coil springs is subjected to unidirectional torsion, so fatigue propagates on a single helical surface. Source: Ref 4

Fig. 18 This broken 30 mm (1.2 in.) diameter steel shaft exhibits flat, relatively smooth fracture, without shear lips and with generally horizontal beach marks, at top and bottom areas. Along with ratchet marks (four distinct ratchet marks are evident along the top edge), these features are consistent with reversed-bending fatigue having multiple origins.

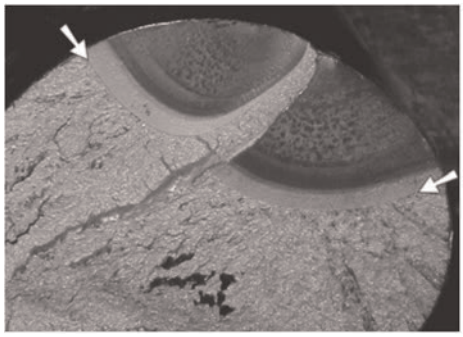

Fig. 19 Oblique view of a 102 mm (4 in.) diameter hardened-steel machine rod that failed by fatigue fracture. Curved beach marks identify two distinct fracture origins, separated by a shear step of overload fracture (light gray). Older parts of fatigue fracture are decorated by corrosion product (rust, appears dark in this photograph), but the last bands of fatigue fracture remained clean. Arrows mark the fatigue crack boundaries.

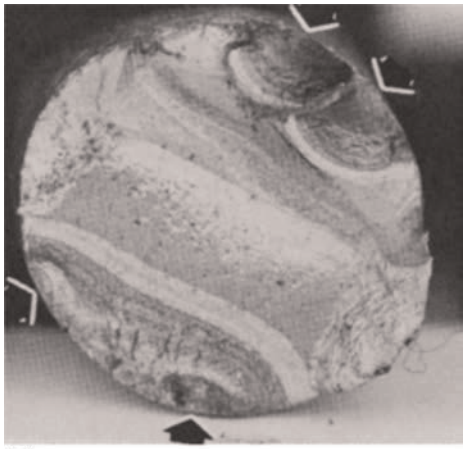

Fig. 20 (a) Beach marks on quenched-and-tempered alloy steel pin fractured in low-cycle fatigue (Ref 4), and (b) arrest lines on a maraging steel stud fractured in the laboratory by stress-corrosion cracking under steady load (Ref 16). The presence of arrest lines is indicative of progressive cracking but not necessarily fatigue.

crack shape, the stress-intensity factor may vary along the crack front, depending on details of the stress distribution (including residual stress) in the crack plane. In macroscopically homogeneous material, fatigue cracks grow faster at points along the crack front of greater stress intensity and slower at points of lower stress intensity, tending toward a shape with uniform stress-intensity distribution. Under uniform tensile loading, in the absence of other factors, the stress-intensity factor is constant along the front of a surface crack with approximately semicircular shape. Consequently, a crack that initiates from a surface point origin in homogeneous material under uniform tension tends to grow with a nearly semicircular crack front. In contrast, under bending, a surface crack tends to develop a shallower shape, because the through-thickness bending-stress distribution results in lower stress intensity at the maximum depth of a semicircular crack. These issues are addressed further in Ref 17.

In general, at least for initial stages of growth, surface fatigue crack fronts tend to have their center of curvature directed toward the initiation site (Fig. 21). Individual fatigue origin sites can be located by tracing the pattern of curved beach marks back to the center of curvature (Fig. 22). In contrast, Fig. 23 illustrates how stress patterns in rotating bending of a notched shaft can result in beach marks that curve away from multiple origin sites. Due to the stress concentration associated with the notch, the fatigue crack propagates more rapidly around the shaft circumference than in the inward direction, resulting in beach marks that are convex to the origins. A change in beach-mark curvature can also be exhibited after extensive crack growth from an individual origin in rotating bending (Fig. 24). The patterns of beach marks expected in cylindrical and rectangular components under various loading conditions have been summarized in widely published diagrams, as illustrated in Fig. 25.

Although macroscopic examination frequently provides valuable information for identifying the presence, extent, and location of fatigue cracking, useful macroscopic features are not always present. For some materials, such as relatively brittle gray cast iron (Fig. 26) or composites (see the section "Fatigue of Polymers and Polymer-Matrix Composites" in this article), there may be no distinct difference between monotonic overload and fatigue appearances. In addition, postfracture mechanical damage (such as rubbing) or corrosion can destroy or obscure original macroscopic features. Ratchet marks are sometimes the last macroscale fatigue fracture features to be destroyed by postfracture damage.

When present, beach marks provide valuable information, including point of origin and crack dimensions at final failure. Beach marks can occasionally be directly linked to component service history. For example, beach marks formed during idle periods of normally operating machinery can sometimes be correlated with the history of outages, or beach (arrest) marks produced by high-stress events in variable amplitude loading may be correlated with the loading spectrum.

Final Overload Fracture

For common component geometries and loading situations, the driving force for fatigue increases as the fatigue crack lengthens and the fatigue crack growth rate increases. When the fatigue crack (or cracks) reaches critical size, the remaining intact ligament fails by overload (fast) fracture. The relative extent of fatigue versus overload fracture regions depends on the nature and level of applied load, geometry, and material toughness. In general, for a given material, the lower the load, the smaller the area of overload fracture (i.e., as nominal stress decreases, the extent of fatigue cracking prior to final failure tends to increase). This behavior is illustrated schematically in Fig. 25.

Features of the overload fracture in a fatigue failure are characteristic of notched or precracked fracture in the subject material. For example, relatively thick, tough material

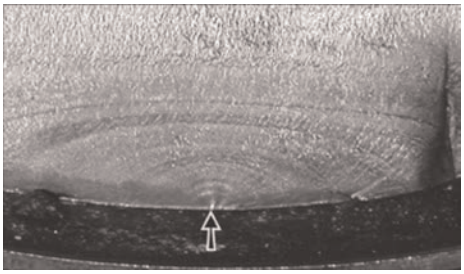

Fig. 21 Curved beach marks are centered on the surface origin (arrow) of this shaft that failed in rotating-bending fatigue. Beach marks are nearly semicircular near the origin. As the crack became larger, it grew more rapidly near the surface where bending stress was highest, resulting in semielliptical beach marks.

Fig. 22 Bolt fracture surface produced by unidirectional bending fatigue. The origin site can be located by tracing the centers of curvature of beach marks back to the thread root at the arrow. Source: Ref 4

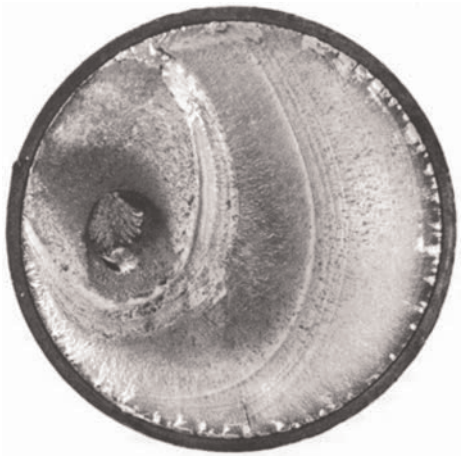

Fig. 23 Carbon steel shaft broken in rotating-bending fatigue. Fatigue fracture initiated at numerous sites along a sharp snap ring groove; ratchet marks appear as shiny spots along the surface. Cracks coalesced into a single fatigue crack that—due to the bending-stress distribution—grew most rapidly near the surface, resulting in beach marks that curve away from the origin sites toward the area of final overload fracture at left. Source: Ref 11

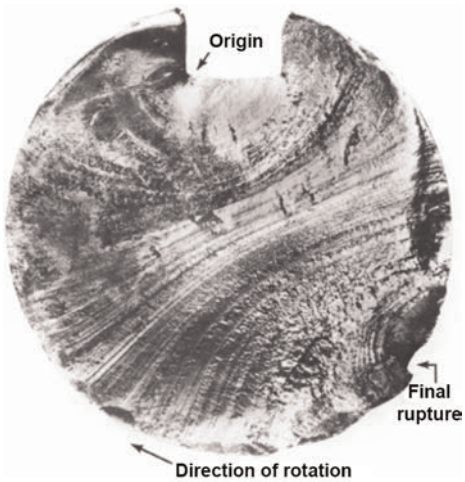

Fig. 24 Rotating-bending fatigue failure of keyed medium-carbon steel shaft. Fatigue initiated at a corner of the keyway, as marked. Beach marks in that vicinity are concentric about the origin. As the fatigue crack grew, the bending-stress distribution produced more rapid growth near the shaft surface. Consequently, beach marks in the later stages of life curved toward the final overload zone. Roughness of the fracture surface also increased nearer the final overload zone. Source: Ref 11

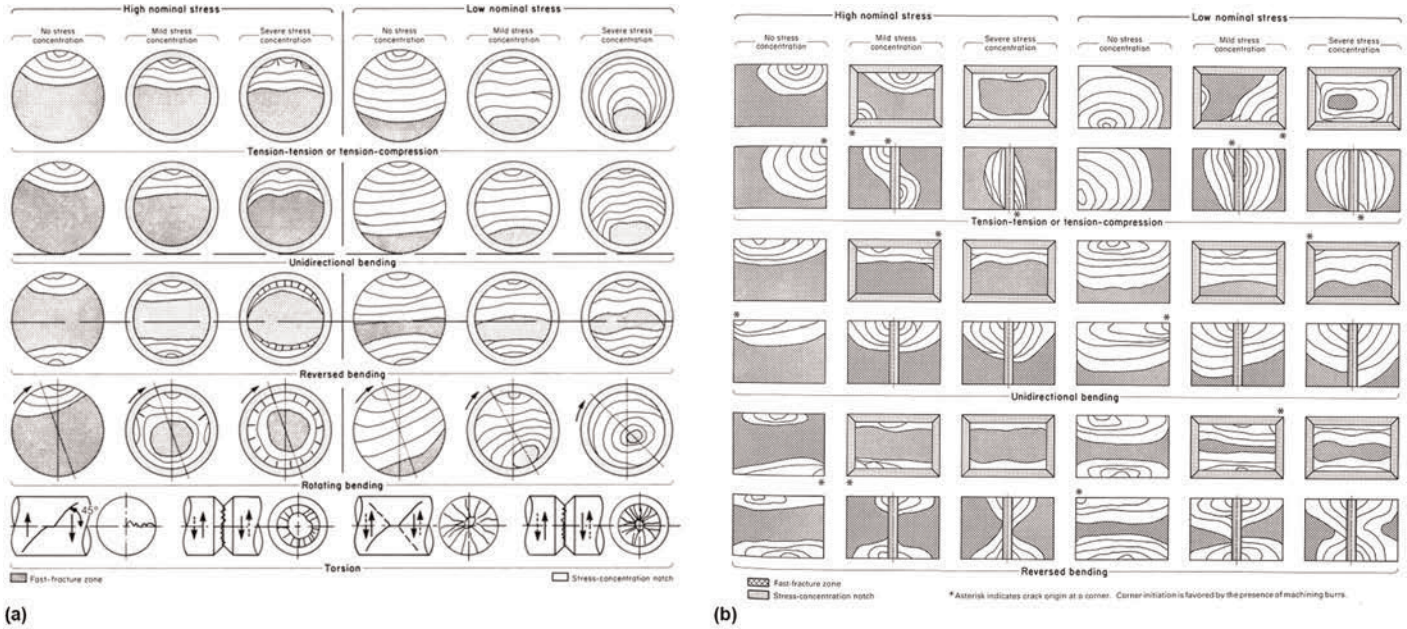

Fig. 25 (a) Schematic diagrams illustrating characteristic patterns of fatigue beach marks, ratchet marks, and relative extent of fast overload fracture in cylindrical components subjected to various loading and notch conditions. (b) Schematic representation of fatigue fracture surface marks produced in square and rectangular components and in thick plates under various loading conditions. Source: Ref 4

loaded in tension across the plane of the fatigue crack will exhibit tensile fracture extending from the fatigue zone and in the same plane, with shear fracture at 45° (i.e., the shear lip) bordering the tensile fracture (Fig. 1). In contrast, overload fracture extending from the fatigue zone in relatively thin sheets of tough material tends to occur on one or two slant planes oriented at approximately 45° to the loading direction, indicative of ductile overload.

In some situations, the zone of slow fatigue crack growth can be followed by a region where increments of unstable (overload) crack extension are separated by bands of progressive fatigue fracture (Ref 18) (Fig. 27). The occurrence of such increments of overload fracture is often associated with variable amplitude or spectrum loading in relatively ductile material.

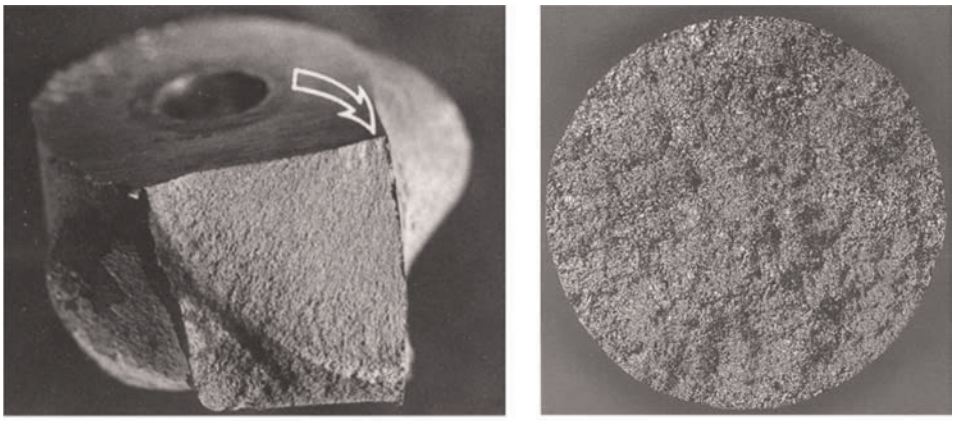

Fig. 26 Fatigue cracks in laboratory test specimens. (a) Steering knuckle made of ferritic ductile iron showing macroscopic features of a fatigue crack initiated at a sharp corner. (b) Rotating-bending fatigue specimen made of as-cast gray iron. Fatigue in this relatively brittle gray iron is macroscopically indistinguishable from overload fracture. Source: Ref 7

Corrosion Fatigue

The presence of a corrosive environment can detrimentally affect fatigue performance, and the effect can be marked. Corrosion can enhance fatigue crack initiation (e.g., by reducing the number of cycles to initiate at a given stress or by lowering the stress required to initiate fatigue) and can increase fatigue crack growth rates.

Corrosion can contribute to fatigue crack initiation through the formation of pits, which then act as geometric stress raisers (Fig. 28). Corrosion pitting evident on mating surfaces at the fatigue crack origin is consistent with a corrosion fatigue role, but the analyst must recognize that wastage can occur postfracture as well. Corrosion can contribute to the formation of beach marks, and fatigue fracture regions are often decorated by corrosion product that is more extensive on older parts of the fatigue region and absent or less voluminous on the final overload fracture zone (Fig. 19).

Macroscopic Features Mistaken for Fatigue

Service failures can exhibit fracture surfaces with macroscopic features similar or identical to those produced by fatigue crack propagation, when fatigue was not the actual fracture mechanism. For example, as described previously, arrest lines can be produced by other progressive fracture mechanisms, such as stress-corrosion cracking. Such progressive fractures, similar to fatigue, are typically oriented normal to the direction of tensile stress and lack gross plastic deformation.

Features not associated with slow progressive cracking have also been mistakenly identified as beach marks. Rib marks, break wave markings (Ref 20), and Wallner lines in brittle materials such as glass and rigid plastics have a curved pattern outlining successive positions of the crack front. However, these markings are produced by interaction of stress waves

with a rapidly moving overload crack and are not indicative of progressive stable crack growth (Ref 21) (Fig. 29, 30). Similarly, curved ridges can form during ductile overload of low-alloy steel (Fig. 31). Transitions in fracture mechanism or morphology (e.g., from ductile microvoid formation to cleavage fracture) can also produce curved marks on fracture surfaces. Such transitions can be caused, for example, by changes in underlying microstructure. The presence of marks such as these does not denote progressive fatigue fracture.

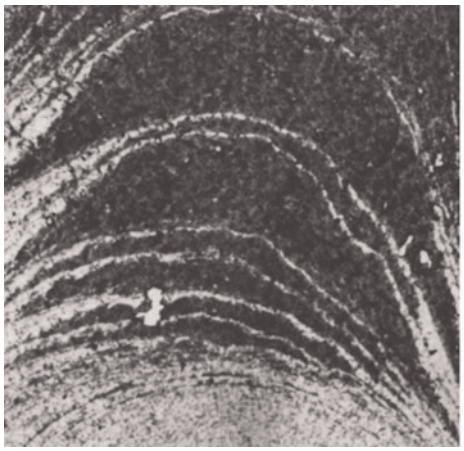

Fig. 27 Discrete bands of fast overload fracture (dull gray) separated by bands of progressive fatigue fracture (bright gray) on service fatigue failure of forged aluminum alloy. Image made by transmitting light through a plastic replica of the fracture surface. Source: Ref 16

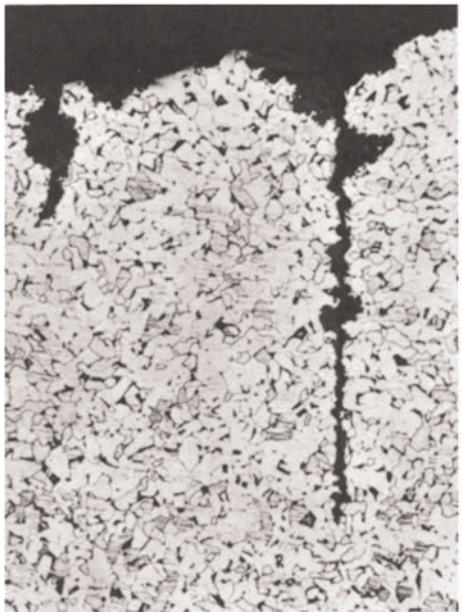

Fig. 28 Metallographic cross section (nital etched) through carbon steel boiler tube. Corrosion fatigue cracks have initiated from the base of pits. Source: Ref 19

Microscopic Appearance of Fatigue Fracture in Metals

Microscopic examination of fracture surfaces can disclose features related to mechanism, type of loading, and contributing factors (e.g., environmental, manufacturing, and material influences) that cannot be discerned macroscopically. While readily identifiable microscopic features associated with fatigue of particular materials exist, not all materials display the same characteristics, and not all materials exhibit a unique fatigue morphology.

Examination of fracture features by light microscopy is limited by resolution and depth of field capabilities. Fine features cannot be resolved, and the height of important features on fracture surfaces often exceeds optical depth of field, especially at higher magnifications.

Electron microscopes have been used to study fracture of materials since the 1950s, and scanning electron microscopes (SEMs) have been commercially available since 1965 (Ref 23). Today (2020), the SEM is standard equipment for any laboratory performing failure analysis and fractography. The SEM offers significantly superior resolution and depth of field compared to light microscopes, markedly increasing the useful magnification range. Compared to transmission electron microscopes, the SEM permits examination of relatively large samples and produces images with a three-dimensional character.

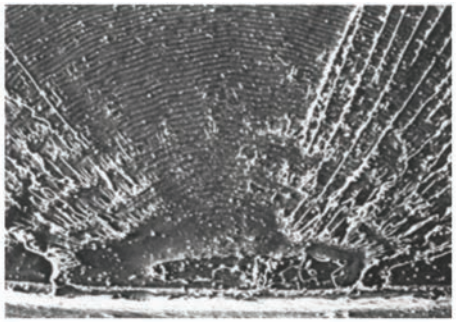

Fig. 29 Low-magnification view of fracture origin area of polycarbonate impact test specimen. Curved Wallner lines, formed by interaction between the rapidly progressing crack front and dynamic stress waves, are reminiscent of beach marks but do not indicate progressive fatigue fracture. Source: Ref 22

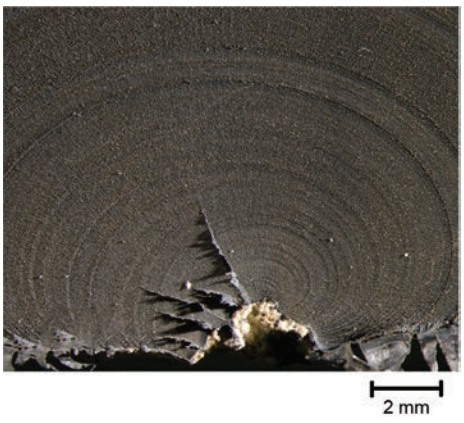

Fig. 30 Fracture of an old polyethylene pipe showing rib marks curving toward the fracture origin. Courtesy of D. Edwards

Striations

Striations are a classic microscopic feature of fatigue in metals. The dictionary defines striations as a series of parallel grooves or lines. In this article, the narrower, commonly used definition of fatigue striation is used: a striation is a microscopic groove or furrow that delineates a local fatigue crack front after a single cycle of loading. Figure 32 illustrates the correlation between striations and loading. Determination that particular marks are striations, and consequent identification of characteristic appearance, has been accomplished by comparing striation spacing with macroscopic measurements of fatigue crack growth rate.

Well-defined fatigue striations form in certain materials under appropriate stress ranges, particularly in metals with multiple active slip planes. For example, well-defined striations are frequently observed at intermediate growth rates in metals such as wrought aluminum and austenitic stainless steel. Examples of fatigue striations are presented in Fig. 32 to 36.

Because each striation corresponds to one loading cycle, the fatigue crack growth rate can be estimated from the spacing between true fatigue striations. Even under controlled conditions, measured striation spacings within a region of macroscopically constant fatigue crack growth rate can vary severalfold.

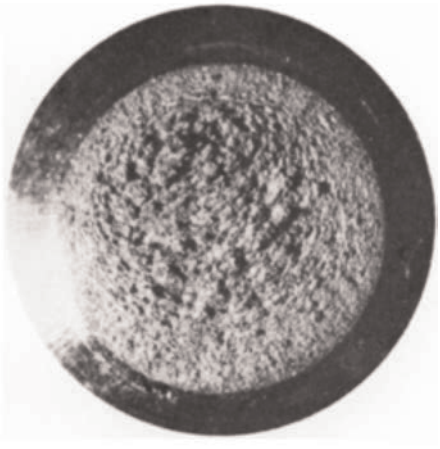

Fig. 31 Fracture surface of notched tension test of alloy steel tested at 0 °C (32 °F). Fibrous overload fracture surface exhibits fine circumferential ridges. Similar markings have been erroneously identified as fatigue beach marks. Source: Ref 16

Multiple striation spacing measurements must therefore be made to obtain reliable sampling. For correlation with applied stress intensity or load, the location at which striation spacing is measured must be well established. Small loads may not produce resolvable striations. This must be considered in circumstances involving total cycle counts for variable amplitude loading. Therefore, any attempt to count striations and relate them to life cycles of the part or equipment must be done with care (Ref 24).

The presence of true fatigue striations is unambiguous and indisputable evidence of fatigue crack propagation. However, depending on material and loading conditions (as well as condition of the fracture surface), the absence of striations may not mean that fatigue did not occur. Not all metals form distinct striations in fatigue, and those that do may not form striations under all stress ranges. Examples of other microscopic fatigue morphologies are presented subsequently, followed by some examples of striation-like features that have been mistaken for true striations.

Ill-Defined Striations and Other Characteristic Appearances

Many common steels and other alloys either exhibit ill-defined (unclear) striations under fatigue crack growth or have characteristic fatigue features without discernable striations. However, the fatigue fracture surface morphology is generally recognizable and often

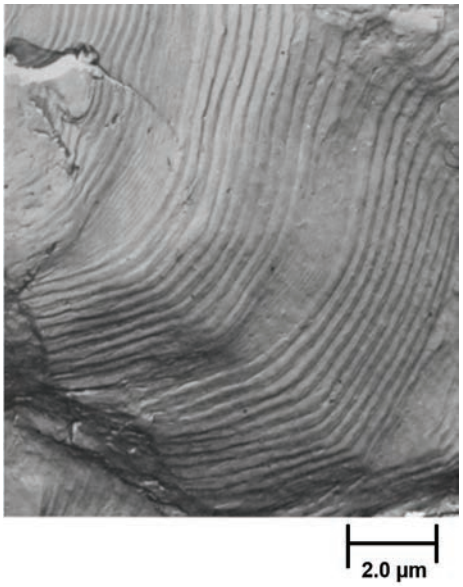

Fig. 32 Transmission electron fractograph of aluminum alloy laboratory spectrum loading fatigue test. Striation spacing varies according to loading, which consisted of ten cycles at a high stress alternating with ten cycles at a lower stress. The fracture surface exhibits bands of ten coarse striations alternating with bands of ten fine striations. Source: Ref 16

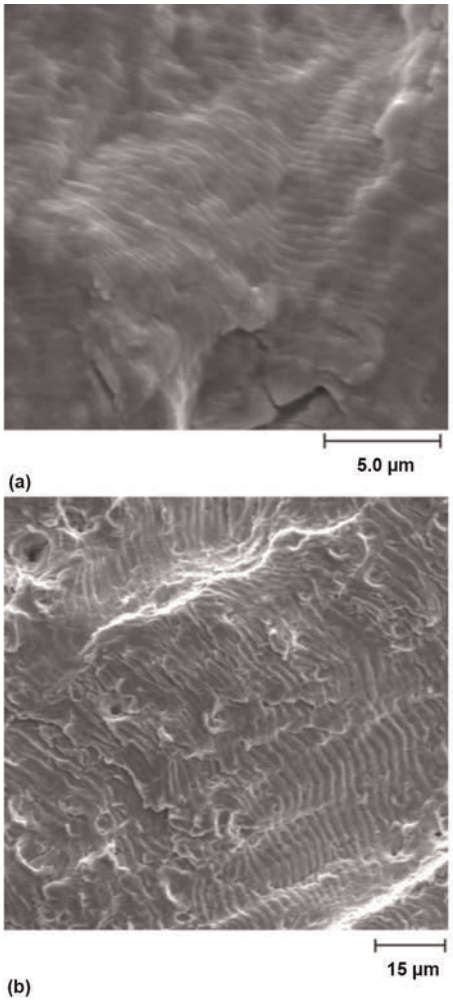

Fig. 33 Fatigue striations in 18-8 austenitic stainless steel tested in rotating bending. (a) Fine striations were located midway between origin and final overload fracture, while (b) coarse striations were located closer to the overload area. Overall direction of crack growth in these scanning electron microscopy views is from lower left to upper right.

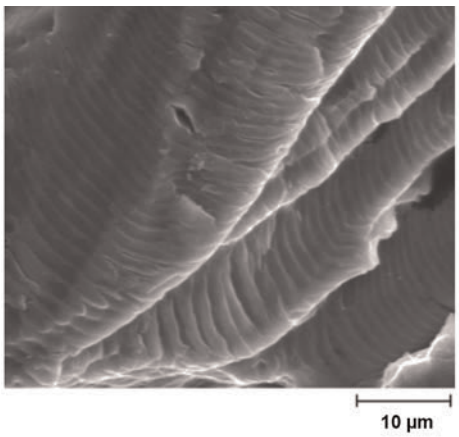

Fig. 34 Scanning electron microscopy view of fatigue striations in aluminum forging tested under cyclic loading

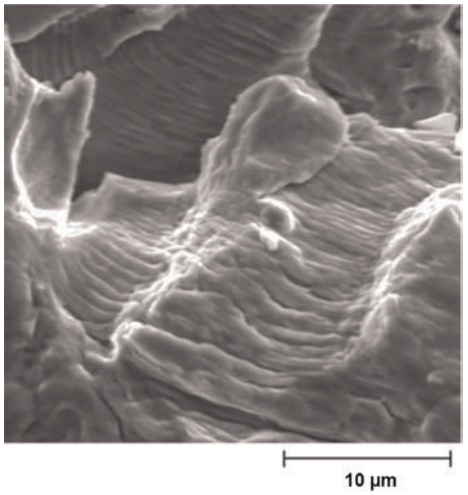

Fig. 35 Striations observed by scanning electron microscopy on rotating-beam fatigue specimen made of cold-worked electrolytic tough pitch copper. Crack growth direction is from upper right to lower left, and specimen was tested at relatively high stress.

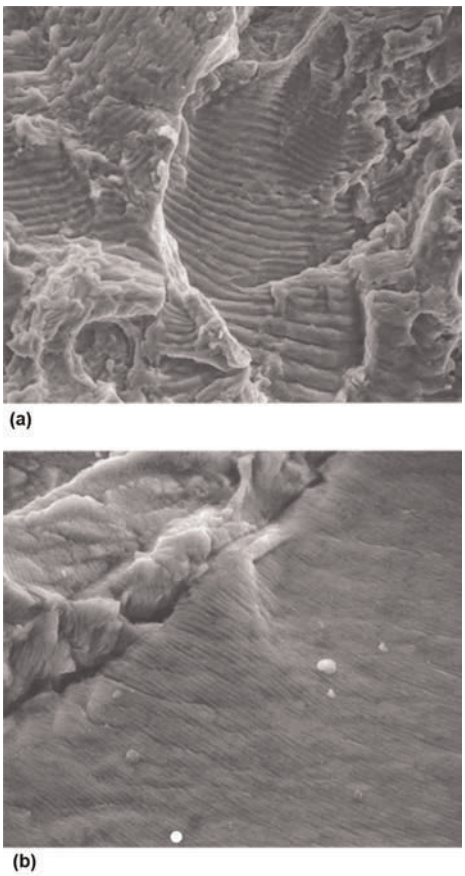

Fig. 36 (a) Coarse and (b) fine striated morphology observed on fatigue of a hot isostatically pressed titanium alloy. Source: Ref 7

displays parallel microcracks. Examples of characteristic fatigue features in steels are presented in Fig. 37 and 38. See the article "Fracture Appearance and Mechanisms of Deformation and Fracture" in this Volume for more details.

Crystallographic Fatigue

Fatigue fracture of metals with low stacking fault energy, which favors planar slip, can occur over extended areas along crystallographic planes, producing a faceted appearance. For example, a cobalt-base alloy used in medical implants exhibits crystallographic fracture in laboratory fatigue testing at all levels of applied load (Ref 25) (Fig. 39). No striations were found. Many nickel-base superalloys can also fatigue with this faceted appearance over large regions.

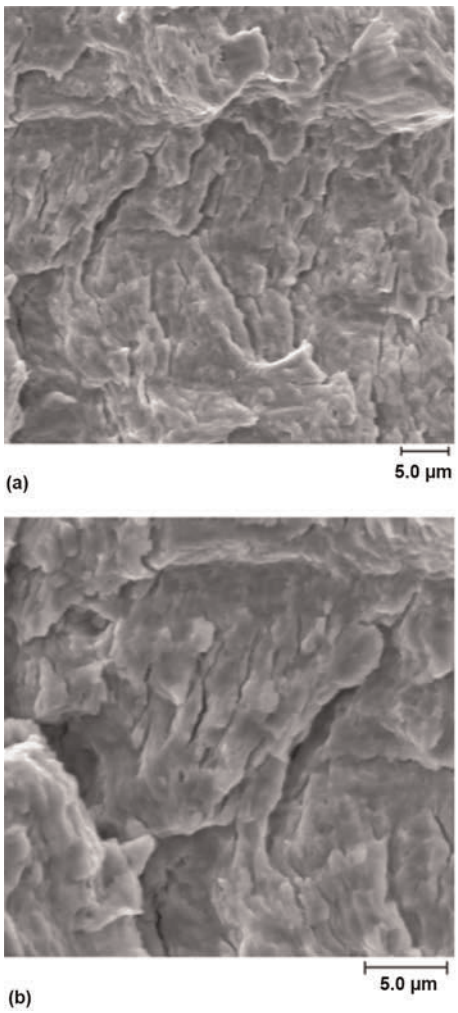

Fig. 37 Two views at different magnifications showing fatigue appearance characteristic of many steels. Striations are not resolved or are ill-defined. Quenched-and-tempered medium-carbon alloy steel tested in rotating bending, imaged using a scanning electron microscope

Metals such as austenitic stainless steel (Fig. 40) and aluminum (Fig. 41) fracture crystallographically under conditions of very-low-stress, high-cycle fatigue (i.e., propagation at low ΔK near the fatigue threshold). Flat facets can also appear at near-threshold fatigue crack growth rates in materials such as carbon steel (Fig. 42).

Intergranular Fatigue

Some metals can exhibit fatigue crack propagation along grain boundaries or grain-boundary regions. For example, mixed intergranular/transgranular fracture of a nickel-copper alloy has been reported (Ref 26) (Fig. 43). Copper can also exhibit intergranular fracture in fatigue (Ref 27) (Fig. 44). Some alloys that exhibit transgranular fracture at intermediate fatigue crack growth rates, with more-or-less distinct striations, display regions of intergranular fracture at low (near-threshold) growth rates (e.g., quenched-and-tempered steel) (Ref 28).

Near-eutectoid steel with a narrow, continuous network of ferrite outlining prior-austenite grain boundaries can exhibit intermittent discontinuous areas of fatigue fracture along the ferrite network (Ref 29). Fatigue fracture within these ferrite layers is reportedly flat and featureless.

Fatigue crack propagation in most structural alloys is typically transgranular. However, in some alloys environmental factors can contribute to intergranular fatigue. For example, corrosion fatigue of alloy steel tested in humid air can occur intergranularly.

High Growth Rates

As a fatigue crack approaches critical size, the growth rate generally increases. Monotonic overload features often appear on the progressive fracture surface. For example, isolated cleavage facets are present on pearlitic steel fatigue fracture surfaces formed at high growth rates (Fig. 45). Depending on alloy and condition, microvoids and intergranular fracture can also appear in high-growth-rate fatigue.

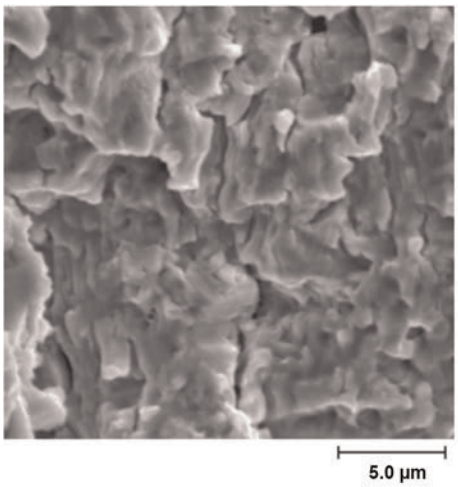

Fig. 38 Scanning electron microscope view of fatigue fracture surface of annealed medium-carbon alloy steel tested in rotating bending. No distinct fatigue striations could be resolved. Crack growth direction from right to left

Microscopic Features Mistaken for Fatigue

Inexperienced or uninformed analysts too frequently interpret any set of roughly parallel markings observed in an SEM during examination of a fracture surface as fatigue striations. Features such as postfracture mechanical damage often exhibit fine, parallel marks or

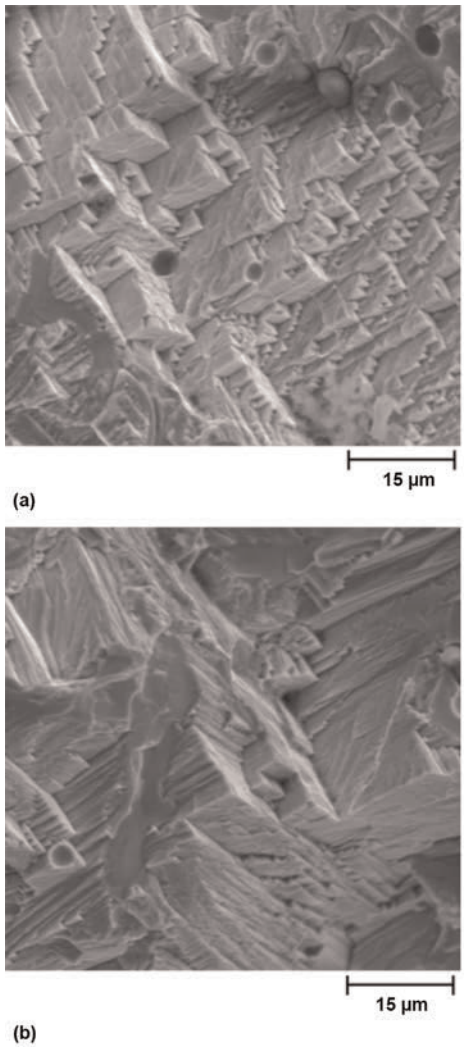

Fig. 39 Crystallographic fatigue in fracture mechanics specimen of cast Co-Cr-Mo-C medical implant alloy. Scanning electron microscope views located (a) 0.025 mm (0.001 in.) from machined notch tip and (b) 7.6 mm (0.3 in.) from notch tip. Fatigue striations were not resolvable at any location, and the entire fatigue fracture surface displayed similar crystallographic features. Courtesy of D.O. Cox, Cox and Company

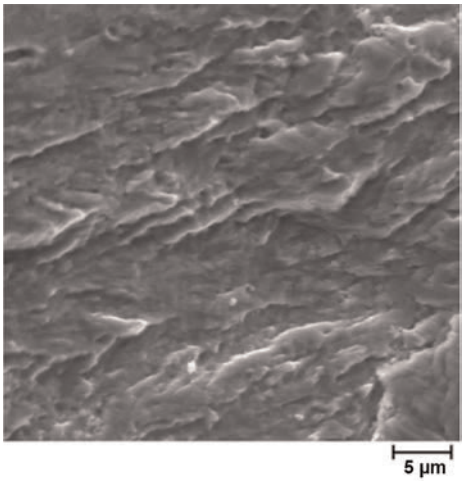

Fig. 40 Crystallographic fatigue of 18-8 austenitic stainless steel near fracture origin in rotating-beam specimen. Global crack propagation direction from lower left to upper right in this scanning electron microscope view

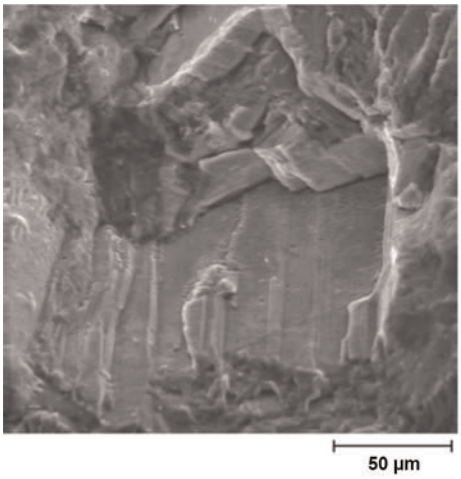

Fig. 41 Crystallographic fatigue of 6000-series aluminum extrusion near fracture origin in rotating-beam specimen. Global crack propagation direction from bottom to top in this scanning electron microscope view

scratches (Fig. 46). Overload fracture of relatively tough and ductile materials can display fine, local markings produced by slip processes associated with monotonic loading. Such slip traces, known as serpentine glide, are illustrated in Fig. 47. Underlying microstructure can influence fracture paths. For example, fracture of pearlitic steel in fatigue or overload can contain patches of parallel marks formed by the influence of underlying pearlite lamellae.

As noted previously, near-threshold fatigue cracking of austenitic stainless steel can be crystallographic. Chloride-induced transgranular stress-corrosion cracking of austenitic stainless steels exhibits cleavage-like features (Ref 30). Distinction between these fracture modes by fractography is difficult or impossible, and

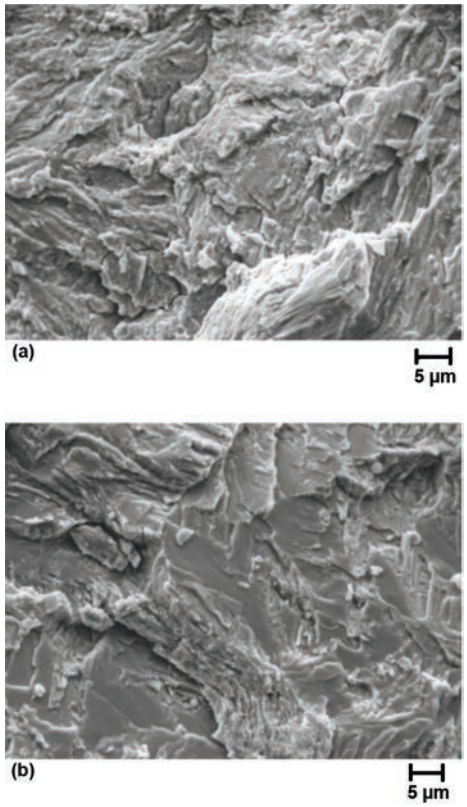

Fig. 42 Fully pearlitic steel fatigue fracture surfaces. Crack growth direction is from left to right in both images. (a) Intermediate crack growth rate (~0.1 µm/cycle). (b) Low crack growth rate (~0.001 µm/cycle). No fatigue striations were resolved by scanning electron microscopy at any crack growth rate. Unmarked facets are more prevalent at low (near-threshold) growth rates.

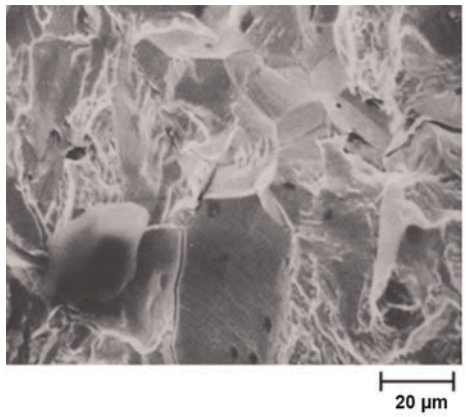

Fig. 43 Scanning electron microscope view of laboratory fatigue fracture of a 70-30 nickel-copper alloy showing mixed intergranular and transgranular morphology. Source: Ref 26

proper identification requires knowledge of service conditions.

As a rule, true fatigue striations never intersect or cross over each other. Furthermore, striation spacing ranges from 10^{-9} to 10^{-6} m; therefore, a minimum magnification of 600×

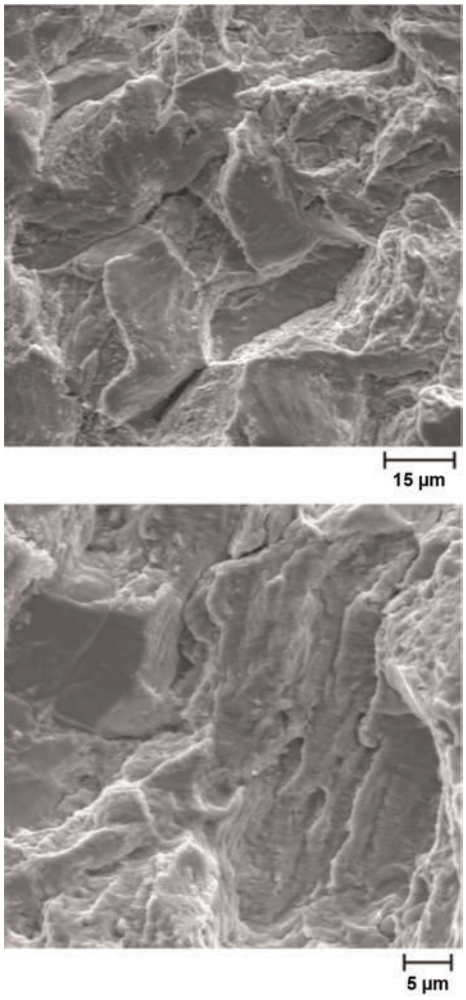

Fig. 44 Scanning electron microscope views of intergranular facets within fatigue crack propagation area of cold-worked electrolytic tough pitch copper tested in rotating bending at moderately low stress

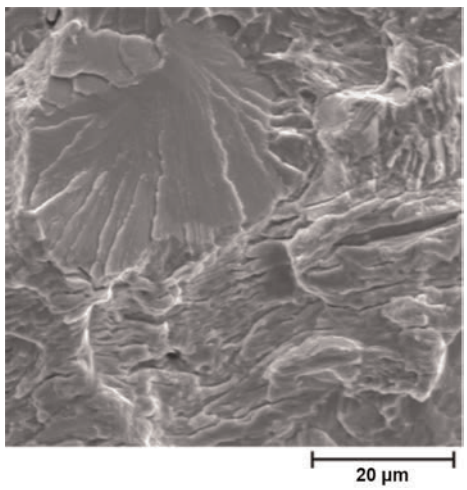

Fig. 45 Isolated cleavage facet within progressive high-growth-rate fatigue fracture of fully pearlitic steel, as viewed in the scanning electron microscope

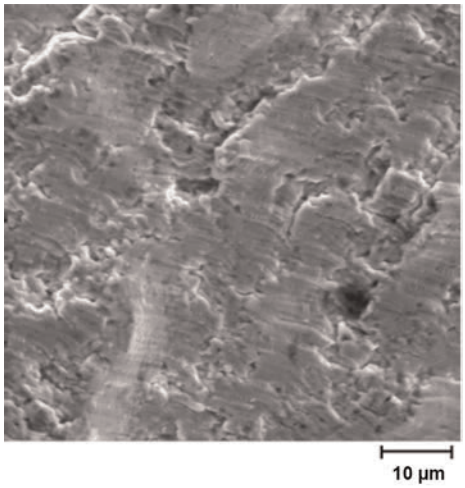

Fig. 46 Postfracture mechanical damage can exhibit fine, parallel markings, as illustrated in this scanning electron microscope view of a steel sample.

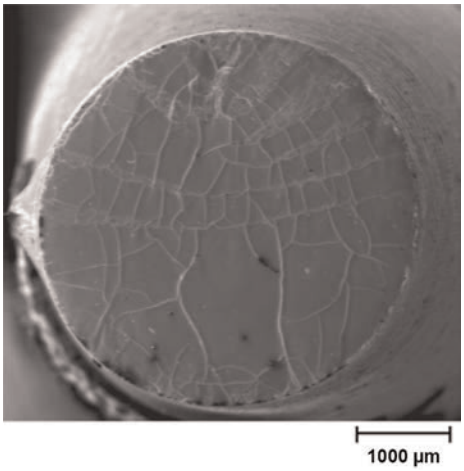

Fig. 48 Artifacts generated by improper platinum sputter coating of a 4.6 mm (0.18 in.) diameter polycarbonate rotating-beam fatigue specimen. This scanning electron microscope view shows a pattern in the coating reminiscent of "mud-cracking."

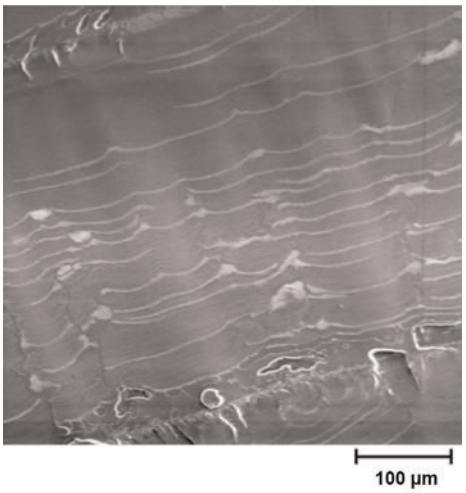

Fig. 50 Features observed on fatigue area of polymethyl methacrylate rotating-beam specimen. Sample was sputter coated with platinum for scanning electron microscopy examination.

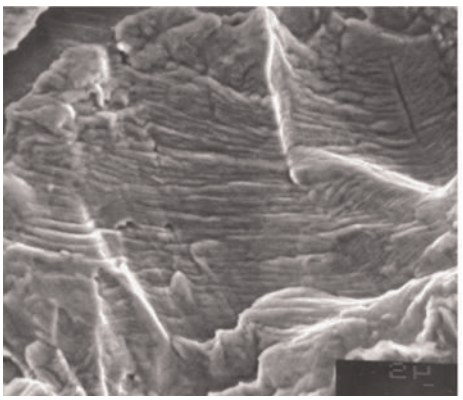

Fig. 47 Scanning electron microscope view of serpentine glide on elevated-temperature (650 °C, or 1200 °F) laboratory tension test of nickel-molybdenum alloy. Although similar in appearance, these markings are not fatigue striations.

Fig. 49 Scanning electron microscope view of fatigue striations in medium-density polyethylene, laboratory tested at 0.5 Hz with maximum stress 30% of the yield strength. Crack growth is upward in this view. Original magnification: 200×. Source: Ref 4

is needed to resolve striation spacing. In practice, magnifications of 1000 to 3000× are needed for comfortable resolution and imaging of fatigue striations. Any striation-like features observed at magnifications below approximately 500× are most likely not true fatigue striations.

Fatigue of Polymers and Polymer-Matrix Composites

Exemplar SEM fractographs of polymers are provided in Ref 9, and fractography of fatigue in engineering plastics is included in Ref 21 and 31. Macroscopic features of fatigue of structural polymers can parallel those of metals in many circumstances: relatively flat and smooth fracture, ratchet marks, and overload region. Beach marks are far less common with polymers. While metallic materials readily display crack-arrest lines created by oxidation or crevice corrosion, polymers generally do not.

Because most polymers are not electrically conductive, they must be coated with a thin conductive layer, such as carbon or gold, to allow examination using a standard SEM. The coating is applied by a method such as vacuum evaporation or sputtering. Coating must be performed carefully to avoid damaging the fracture surface (e.g., by excessive heating) or introducing artifacts associated with the coating process (Fig. 48). The need to coat polymer fracture surfaces can be avoided by using an SEM with low-vacuum capability. Scanning electron microscope fractographs of polymer fatigue are presented in Fig. 49 to 51. Unlike metals, which require the use of an SEM and magnifications in excess of 500×, fatigue striations in polymers can often be observed at lower magnifications (e.g., <100×) using a stereomicroscope.

The properties of polymers result in fatigue behavior different from that ordinarily encountered in metals. Except at elevated temperature or in corrosive environments, fatigue of structural metals depends on the number (and magnitude) of loading cycles rather than time under load. However, because of time and rate sensitivity (i.e., viscoelastic behavior) of many polymers at near-ambient temperatures, fatigue depends not only on the number of cycles at a given stress or stress-intensity level but also on frequency and time history of loading (Ref 32). Heat resulting from mechanical hysteresis during cyclic loading of plastics can cause thermal failure.

Additionally, depending on load level and time history, fatigue cracks in polymers may not propagate steadily (with an increment of growth for each fatigue cycle) but may grow in bursts or spurts (Ref 32). These spurts or discontinuous growth bands are associated with a large number of cycles (Ref 31). They can produce microscopic markings that appear very similar to striations but which do not correspond to single load cycles. Consequently, without companion laboratory fatigue crack growth rate data and careful fractographic evaluation, estimation of service history from the spacing between fracture markings can be problematic (Ref 31). Some polymers, such as polycarbonate and polymethyl methacrylate, can exhibit either true striations or discontinuous growth bands, depending on load levels and loading history.

A brief discussion of the fractography of fiber-reinforced, polymer-matrix structural composites is provided in Ref 33. According to that article, fractography of fatigue failures in composite materials can be more difficult than for other materials, such as metals. There may be little macroscopic difference between interlaminar fracture features formed by

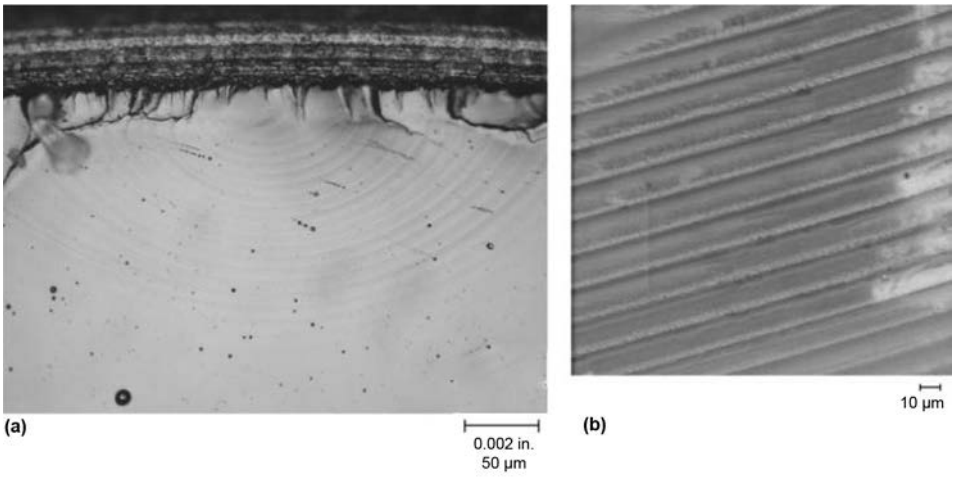

Fig. 51 Features observed on fatigue area of polycarbonate rotating-beam specimen. (a) Optical view at base of notch. (b) Higher-magnification electron fractograph. Sample was sputter coated with platinum for scanning electron microscopy examination.

fatigue and those formed in overload. Composite materials may lack visual indications of the initiation site. Although microscopic fatigue striations may form, areas exhibiting striations are usually isolated and limited in extent. For similar reasons, fatigue striations are generally not visible in heavily filled polymers.

ACKNOWLEDGMENT

Revised from R.A. Lund and S. Sheybany, Fatigue Fracture Appearances, *Failure Analysis and Prevention*, Volume 11, *ASM Handbook*, ASM International, 2002, p 627–640

REFERENCES

1. R. Stephens, A. Fatemi, R. Stephens, and H. Fuchs, *Metal Fatigue in Engineering*, 2nd ed., John Wiley & Sons, 2001
2. J.A. Collins, *Failure of Materials in Mechanical Design; Analysis, Prediction and Prevention*, 2nd ed., John Wiley & Sons, 1993
3. S. Suresh, *Fatigue of Materials*, Cambridge University Press, 1991
4. *Fractography*, 12, *Metals Handbook*, 9th ed., ASM International, 1987
5. S. Bhattacharyya, V.E. Johnson, S. Agarwal, and M.A.H. Howes, Failure Analysis of Metallic Materials by Scanning Electron Microscopy, *IITRI Fracture Handbook*, IIT Research Institute, 1979
6. L. Engel and H. Klingele, *An Atlas of Metal Damage*, Prentice-Hall, 1981
7. G.W. Powell, S. Cheng, and C.E. Mobley, Jr., *A Fractography Atlas of Casting Alloys*, Battelle Press, 1992
8. J. Aleszka, Y. Kim, J. Scott, and A. Kumar, "Fracture Characteristics of Structural Steels: Reference Manual," Technical Report M-258, U.S. Army Construction Engineering Research Laboratory, 1979
9. L. Engel, H. Klingele, G.W. Ehrenstein, and H. Schaper, *An Atlas of Polymer Damage*, Prentice-Hall, 1981
10. G. Parrish, *The Influence of Microstructure on the Properties of Case-Carburized Components*, American Society for Metals, 1980
11. D.J. Wulpi, *Understanding How Components Fail*, 2nd ed., *ASM International*, 1999
12. L.E. Alban, *Systematic Analysis of Gear Failures*, American Society for Metals, 1985
13. F.B. Stulen and W.C. Schulte, Fatigue Failure Analysis and Prevention, *Source Book in Failure Analysis*, American Society for Metals, 1974
14. J. Schijve, Fatigue Crack Growth Under Variable-Amplitude Loading, *Fatigue and Fracture*, Vol 19, *ASM Handbook*, ASM International, 1996, p 110–133
15. Fatigue Failures, *Failure Analysis and Prevention*, Vol 11, *Metals Handbook,* 9th ed., American Society for Metals, 1986, p 102–135
16. *Fractography and Atlas of Fractographs*, Vol 9, *Metals Handbook*, 8th ed., American Society for Metals, 1974
17. K.S. Ravichandran, Effect of Crack Shape on Crack Growth, *Fatigue and Fracture*, Vol 19, *ASM Handbook*, ASM International, 1996, p 159–167
18. D. McIntyre, Fractographic Analysis of Fatigue Failures, *J. Eng. Mater. Technol. (Trans. ASME)*, Vol 97, July 1975, p 194–205
19. P.S. Pao and R.P. Wei, Corrosion-Fatigue Failures, *Failure Analysis and Prevention*, Vol 11, *Metals Handbook*, 9th ed., American Society for Metals, 1986, p 252–262
20. L. Orr, Practical Analysis of Fractures in Glass Windows, *Materials Research and Standards*, Jan 1972, p 21–23
21. M.D. Hayes, D.B. Edwards, and A.R. Shah, *Fractography in Failure Analysis of Polymers*, Elsevier, 2015
22. P.K. So, Fractography, *Engineering Plastics*, Vol 2, *Engineered Materials Handbook*, ASM International, 1988, p 805–810
23. D.O. Cox, R.A. Lund, and I. Roman, Fractography for Failure Analysis, *Pressure Vessel and Piping Technology—1985—A Decade of Progress*, C. Sundararajan, Ed., The American Society of Mechanical Engineers, 1985, p 1003–1012
24. P.H. DeVries, K.T. Ruth, and D.P. Dennies, Counting on Fatigue: Striations and Their Measure, *J. Fail. Anal. Prevent.*, Vol 10 (No. 2), Aug 2010, p 120–137
25. D.O. Cox, "*The Fatigue and Fracture Behavior of a Low Stacking Fault Energy Co-Cr-Mo-C Casting Alloy Used for Prosthetic Devices*," Ph.D. dissertation, UCLA, 1977
26. R.A. Lund and G.J. Fowler, Intergranular Fracture in Engineering Materials, *International Symposium for Testing and Failure Analysis (ISTFA)*, 1984, p 311–321
27. P.K. Liaw, T.R. Leax, R.S. Williams, and M.G. Peck, Near-Threshold Fatigue Crack Growth Behavior in Copper, *Metall. Trans. A*, Vol 13, Sept 1982, p 1607–1618
28. R.O. Ritchie, Near-Threshold Fatigue Crack Propagation in Ultra-High Strength Steel: Influence of Load Ratio and Cyclic Strength, *J. Eng. Mater. Technol. (Trans. ASME)*, Vol 99, July 1977, p 195–204
29. G.J. Fowler, "*Fatigue Crack Initiation and Propagation in Pearlitic Rail Steels*," Ph. D. dissertation, UCLA, 1976
30. T. Magnin and J. Lepinoux, Metallurgical Aspects of the Brittle S.C.C. in Austenitic Stainless Steels, *Parkins Symposium on Fundamental Aspects of Stress Corrosion Cracking*, S.M. Bruemmer et al., Ed., Minerals, Metals and Materials Society, 1992, p 323–339
31. R.W. Hertzberg and J.A. Manson, *Fatigue of Engineering Plastics*, Academic Press, 1980
32. G.C. Pulos and W.G. Knauss, Nonsteady Crack and Craze Behavior in PMMA Under Cyclical Loading, *Int. J. Fract.*, Vol 93, 1998, p 145–207
33. P.L. Stumpff, Fractography, *Composites*, Vol 21, *ASM Handbook*, ASM International, 2001, p 977–987